

Above room temperature ferromagnetism in Mn-ion implanted Si

M. Bolduc, C. Awo-Affouda, A. Stollenwerk, M. B. Huang, F. G. Ramos, G. Agnello, and V. P. LaBella
College of Nanoscale Science and Engineering, University at Albany-SUNY, Albany, New York 12203, USA
 (Received 10 August 2004; revised manuscript received 13 October 2004; published 4 January 2005)

Above room temperature ferromagnetic behavior is achieved in Si through Mn ion implantation. Three-hundred-keV Mn⁺ ions were implanted to 0.1% and 0.8% peak atomic concentrations, yielding a saturation magnetization of 0.3 emu/g at 300 K for the highest concentration as measured using a SQUID magnetometer. The saturation magnetization increased by $\sim 2\times$ after annealing at 800 °C for 5 min. The Curie temperature for all samples was found to be greater than 400 K. A significant difference in the temperature-dependent remnant magnetization between the implanted p-type and n-type Si is observed, giving strong evidence that a Si-based diluted magnetic semiconductor can be achieved.

DOI: 10.1103/PhysRevB.71.033302

PACS number(s): 75.50.Pp

I. INTRODUCTION

Utilizing the spin of the electron in semiconductor devices holds great potential to provide high-speed device structures.¹ The integration of ferromagnetism into these device structures is needed to couple to electron spin. Diluted magnetic semiconductors (DMS) have been demonstrated as a successful method for integrating ferromagnetism through doping of a semiconductor crystal with an additional transition metal impurity such as Mn.²⁻⁵

Epitaxially grown III-V semiconductors such as Ga_{1-x}Mn_xAs have achieved ferromagnetism with Curie temperatures up to 110 K for ($x \approx 5\%$) and have been successfully utilized as spin aligners in spin-LED devices.^{3,6-10} This success has motivated the search for group-IV-based DMS materials with high Curie temperatures due to their compatibility with conventional integrated circuits. Recently, an epitaxially grown single crystal of Mn_xGe_{1-x} ($x=3.5\%$) achieved a magnetically ordered phase from a long-range ferromagnetic interaction at 116 K;¹¹ epitaxially grown thin films of Ce_xSi_{1-x} ($x=0.5\%$) produced a material with a magnetic susceptibility that displayed spin glass-like behavior around 40 K,¹² and epitaxially grown Mn_xSi_{1-x} ($x=5\%$) thin films produced a material with an anomalous Hall effect (due to internal magnetization) around 70 K.¹³ These findings are also supported by theoretical calculations that have predicted ferromagnetic ordering in group-IV semiconductors.⁴

Ion implantation has also been utilized to achieve ferromagnetism in semiconductor crystals, and it is an attractive technique since it is routinely used in the manufacturing of integrated circuits.¹⁴⁻²⁰ For example, 3 at. % Mn-implanted GaN and GaP achieved Curie temperatures of 270 and 250 K, respectively.¹⁴ Furthermore, ion implantation is attractive for a Si-based DMS, since Mn concentrations of about 1 at. % ($\sim 10^{20}$ cm⁻³ for Si) would be needed, exceeding the solubility limit of Mn in Si ($\sim 10^{16}$ cm⁻³ at 1000 °C).²¹ Some-what surprisingly, the fabrication of a Si-based DMS via ion implantation of Mn has not been reported. Only recently, have the structural properties of Mn-ion implantation into Si been studied.^{22,23} Missing from both the epitaxially grown (Mn, Ce)-doped silicon thin-film studies and the Mn-ion implantation into Si studies is a direct

measure of the ferromagnetic properties and their dependence upon temperature.

In this paper, above room temperature ferromagnetism is measured in Mn-ion implanted Si single crystals. Ferromagnetic hysteresis loops and a Curie temperature greater than 400 K indicate the synthesis of a potentially new DMS material in p-doped or n-doped Si samples. The strength of the ferromagnetism is affected by the Mn concentration, thermal annealing, and carrier type of the Si, while the normalized temperature-dependent behavior up to 400 K is only affected by the carrier type, suggesting that the ferromagnetic exchange is hole mediated.

II. EXPERIMENT

The Mn-implanted Si samples were prepared from commercially purchased single-crystal Si wafers (p-type 10^{19} cm⁻³ or n-type 10^{15} cm⁻³). They were first cleaned in diluted HF for 5 min to remove the native oxide on the surface prior to implantation. The ion implantation was performed with an Extrion 400 at a base pressure of 5×10^{-6} Torr. Mn⁺ ions extracted from a plasma arc source were implanted at an energy of 300 keV at doses of 1×10^{15} cm⁻² and 1×10^{16} cm⁻². The samples were held at 350 °C during implantation to avoid amorphization.¹⁷ Following implantation rapid thermal annealing was performed on some samples at temperature of 800 °C for 5 min in a forming gas of N₂.

Measurements of magnetization vs applied field at 10, 77, and 300 K were performed using a commercially available superconducting quantum interference device (SQUID) magnetometer (Quantum Design MPMS), which had a temperature range from 10 to 400 K. To determine Curie temperature (T_c), the remnant field was measured under a zero applied field after cooling the sample from room temperature. The structural composition was investigated by means of dynamic secondary ion mass spectroscopy (SIMS) depth profiling (Perkin-Elmer PHI 6300 Quadrupole). The measured profiles had a Gaussian shape peaking at 260 nm with a full-width half-maximum (FWHM) of 120 nm in good agreement with Monte Carlo simulations. The Mn concentration was calculated by using the density of Si which gave

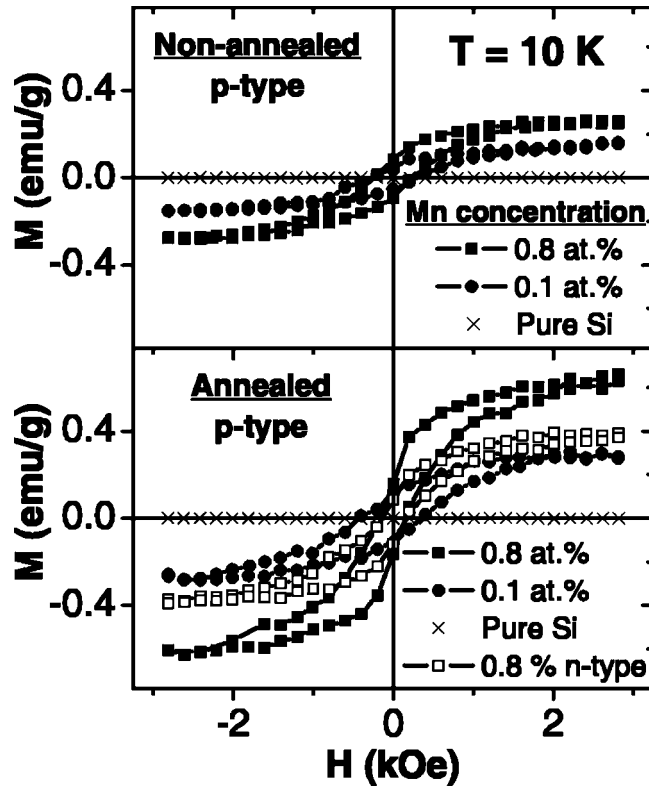


FIG. 1. (top) Ferromagnetic hysteresis loops at 10 K for Mn-implanted p-type Si with no post-implant anneal. (bottom) Hysteresis loops taken at 10 K for Mn-implanted p-type (solid markers) and n-type (open markers) Si after rapid thermal annealing. Data for unimplanted pure Si sample are also shown for comparison.

Mn peak concentrations of 0.1 and 0.8 at. % for the lower and higher implantation dose, respectively. The SIMS depth profiles were calibrated by measuring the crater depth using a stylus profilometer. No detectable contaminant such as Fe was found in either nonannealed or annealed implanted Si wafers as determined by x-ray photoelectron spectroscopy (XPS) or Rutherford back scattering (RBS). Finally, Hall effect measurements on the initial p-type doped samples did not show a significant change in carrier concentration after Mn implantation.

III. RESULTS

Magnetization curves (M vs H) at 10 K for all samples are shown in Fig. 1. Ferromagnetic hysteresis loops are observed in the Mn-ion implanted Si samples. The linear background diamagnetic behavior of the Si was subtracted for all the displayed data. The nonimplanted Si, both before and after annealing, has no net magnetic moment, whereas the saturation magnetization increases with Mn concentration. Post-treatment annealing increases the saturation magnetization by $\sim 2\times$ as displayed in Fig. 1 (bottom). The saturation magnetization is weaker for the implanted n-type Si. The coercive field is ~ 250 Oe for all samples. The mass of the sample was calculated by taking the FWHM of the SIMS profile.

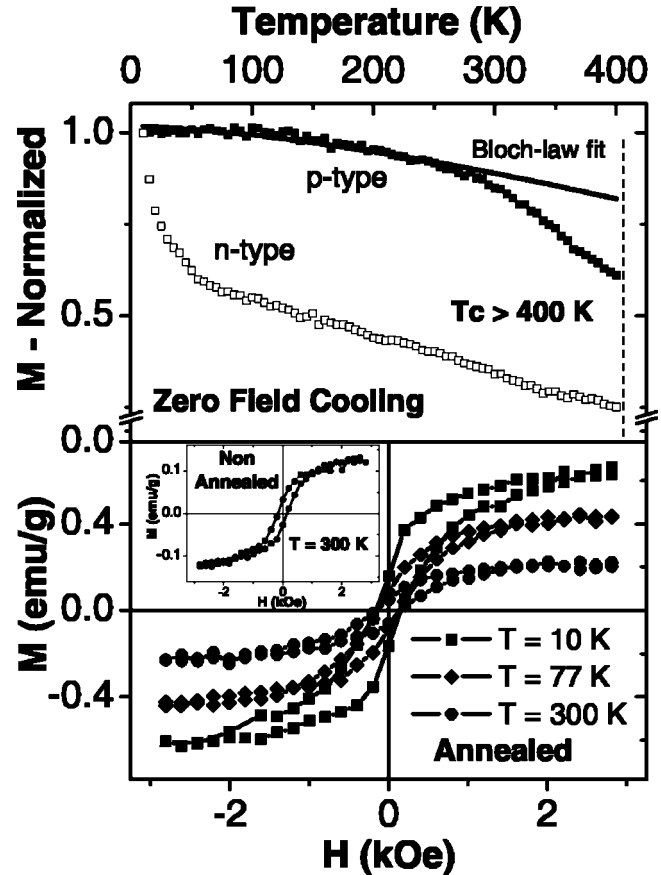


FIG. 2. (top) Temperature dependence of the normalized remnant magnetization for Mn-implanted Si both p-type (solid markers) and n-type (open markers). A Bloch law dependence is fitted (solid line) with 90% confidence. (bottom) Ferromagnetic hysteresis loops at 10, 77, and 300 K from Mn-implanted Si after rapid thermal annealing. The inset shows a ferromagnetic hysteresis loop at 300 K before annealing.

The normalized temperature-dependent remnant magnetization curve [$M_r/M_r(10\text{ K})$ vs T] of 0.8 at. % Mn-ion implanted p-doped and n-doped Si crystals between 10 and 400 K under zero applied magnetic field is shown in Fig. 2 (top). The samples were zero-field cooled from room temperature to 10 K prior to the magnetization measurements. The normalized data for all the p-type doped samples displayed similar temperature-dependent behavior; hence, only the 0.8 at. % Mn-implanted samples are displayed. Ferromagnetic order from 10 to 400 K is observed with the magnetization decreasing to 60% of its initial value at 400 K. A Bloch law dependence ($M \propto T^{(3/2)}$) is fit to the data over the temperature range < 200 K with a 90% confidence. For the n-type sample, an initial rapid decrease of the magnetization with temperature is followed by a much slower decay at temperatures above 50 K, finally reaching 40% of its initial value at 400 K. Hysteresis loops at 10, 77, and 300 K for 0.8 at. % Mn-ion implanted p-doped Si are also presented in Fig. 2 (bottom). The inset shows hysteresis at 300 K of the same sample prior to annealing.

IV. DISCUSSION

Similar to other Mn-doped semiconductors the Mn-implanted Si crystals show ferromagnetic ordering. Ferromagnetic ordering in a DMS arises from the long-range ferromagnetic coupling of the magnetic moments of the sparsely distributed Mn impurities, which overcomes the short-range antiferromagnetic exchange that occurs in bulk Mn. The long-range exchange coupling is also hole mediated and therefore sensitive to the carrier type and carrier concentration. This hole-mediated exchange is demonstrated by the n-type sample having weaker saturation magnetization than p-type, as displayed in Fig. 1. The strength of the saturation magnetization increases $\sim 2\times$ after annealing from 0.3 to 0.6 emu/g for the 0.8 at. % concentration. Annealing heals the damage in the crystal that arises from the implantation process, possibly increasing the strength of the hole-mediated exchange coupling.

The saturation magnetization after annealing of the 0.8 at. % Mn concentration corresponds to a Bohr magneton (μ_B) per Mn atom of $\sim 1.5 \mu_B$, indicating that 30% of the Mn atoms are participating if each Mn atom has the moment of an isolated Mn atom of $5 \mu_B$. For the 0.1 at. % concentration the magnetic moment per Mn atom is very close to $5 \mu_B$, indicating that almost all of the Mn contributes to the exchange coupling. For comparison, almost 60% of Mn contributes in $\text{Mn}_{0.01}\text{Ge}_{0.99}$, and 13% contribute in $\text{Ga}_{0.96}\text{Mn}_{0.04}\text{As}$.^{11,24} The observed decrease in the number of contributing Mn atoms with increasing concentration is strong evidence that the short-range antiferromagnetic coupling is overcoming the long-range interaction due to the closer spacing of the Mn ions.^{4,25} The very large fraction of the Mn ions that contributes when the Mn peak concentration is extremely low (0.1 at. %) indicates that the short-range antiferromagnetic exchange coupling is almost nonexistent. These results suggest that lower concentrations of Mn may be needed in Si when compared to other DMS systems to achieve the optimal magnetic properties.

Most striking is the observation of ferromagnetic ordering well beyond room temperature, indicating that the Curie temperature is greater than 400 K. This behavior is *not* affected by the Mn concentration or thermal annealing. It has been determined that T_c varies with Mn concentration in other DMS systems.^{3,11} However, since T_c is typically assigned to the inflection point which is beyond the temperature limit of the magnetometer, we can only speculate that the T_c remains unchanged across all samples. Below 200 K the magnetization does not show any distinct transition for the p-type

samples, indicating a stable and fully persistent ferromagnetic state as observed by the Bloch law dependence. In contrast, the n-type material exhibits an atypical magnetization curve usually found in weakly coupled systems.²⁵ This behavior further suggests that the ferromagnetic exchange coupling is hole mediated, and is consistent with other DMS systems^{14,26} and theoretical treatments.^{4,25,27}

Of great concern when measuring magnetic properties of implanted semiconductors is the presence of second phases or crystallites and their effect upon the magnetic properties. These second phases or crystallites can give rise to superparamagnetic behavior where a blocking temperature is observed below which the magnetization vanishes in zero-field cooled magnetic measurements.²⁸ Clearly, the temperature-dependent ferromagnetic behavior of this Si:Mn system *does not* have a blocking temperature, and fully saturated hysteresis loops are obtained at 10, 77, and 300 K (cf. Fig. 2). However, further investigation in structural properties is needed to clearly determine the presence of clusters. The ferromagnetic properties may be affected by the formation of crystallites, but the presence of clusters of a few magnetic atoms would not exclude carrier-mediated ferromagnetism.²⁹

V. CONCLUSION

Above room temperature ferromagnetism has been achieved in Mn-ion implanted Si. The structural and magnetic data indicate the formation of a single-crystal material with ferromagnetic ordering. The remnant magnetization and its dependence upon temperature is strongly affected by the dopant type, suggesting that the ferromagnetic ordering is hole mediated. These results indicate that it may be possible to fabricate a Si-based diluted magnetic semiconductor, furthering the potential for Si-based spintronic devices.

ACKNOWLEDGMENTS

The authors are grateful to Z. Ding and P. Thibado from the University of Arkansas (Fayetteville) for Hall effect measurements. Special thanks to J. Reynolds for helpful discussions and K. Dunn for TEM discussions. This work was supported by the National Science Foundation CAREER-DMR-0349108, New York State Office of Science, Technology and Academic Research Faculty Development Program (NYSTAR-FDP-C020095), and MARCO Interconnect Focus Center. M. Bolduc is partially supported by the Natural Sciences and Engineering Research Council (NSERC) of Canada.

¹S. A. Wolf, D. D. Awschalom, R. A. Buhrman, J. M. Daughton, S. von Molnar, M. L. Roukes, A. Y. Chtchelkanova, and D. M. Treger, *Science* **294**, 1488 (2001).

²T. Dietl, H. Ohno, F. Matsukura, J. Cibert, and D. Ferrand, *Science* **287**, 1019 (2000).

³H. Ohno, *Science* **281**, 951 (1998).

⁴T. Dietl, *Semicond. Sci. Technol.* **17**, 377 (2002).

⁵S. J. Pearton, C. R. Abernathy, D. P. Norton, A. F. Hebard, Y. D. Park, L. A. Boatner, and J. D. Budai, *Mater. Sci. Eng., R.* **40**, 137 (2003).

⁶H. Ohno, A. Shen, F. Matsukura, A. Oiwa, A. Endo, S. Katsumoto, and Y. Iye, *Appl. Phys. Lett.* **69**, 363 (1996).

⁷Y. Ohno, D. K. Young, B. Beschoten, F. Matsukura, H. Ohno, and D. D. Awschalom, *Nature (London)* **402**, 790 (1999).

- ⁸H. Akinaga, S. Miyanishi, K. Tanaka, W. van Roy, and K. Onodera, *Appl. Phys. Lett.* **76**, 97 (2000).
- ⁹Y. D. Park, B. T. Jonker, B. R. Bennett, G. Itkos, M. Furis, G. Kioseoglou, and A. Petrou, *Appl. Phys. Lett.* **77**, 3989 (2000).
- ¹⁰X. Chen, M. Na, M. Cheon, S. Wang, H. Luo, B. D. McCombe, X. Liu, Y. Sasaki, T. Wojtowicz, J. K. Furdyna, S. J. Potashnik, and P. Schiffer, *Appl. Phys. Lett.* **81**, 511 (2002).
- ¹¹Y. D. Park, A. T. Hanbicki, S. C. Erwin, C. S. Hellberg, J. M. Sullivan, J. E. Mattson, T. F. Ambrose, A. Wilson, G. Spanos, and B. T. Jonker, *Science* **295**, 651 (2002).
- ¹²T. Yokota, N. Fujimura, Y. Morinaga, and T. Ito, *Physica E (Amsterdam)* **10**, 237 (2001).
- ¹³H. Nakayama, H. Ohta, and E. Kulatov, *Physica B* **302–303**, 419 (2001).
- ¹⁴N. Theodoropoulou, A. F. Hebard, S. N. G. Chu, M. E. Overberg, C. R. Abernathy, S. J. Pearton, R. G. Wilson, and J. M. Zavada, *J. Appl. Phys.* **91**, 7499 (2002).
- ¹⁵M. E. Overberg, B. P. Gila, G. T. Thaler, C. R. Abernathy, S. J. Pearton, N. A. Theodoropoulou, K. T. McCarthy, S. B. Arnason, A. F. Hebard, S. N. G. Chu, R. G. Wilson, J. M. Zavada, and Y. D. Park, *J. Vac. Sci. Technol. B* **20**, 969 (2002).
- ¹⁶A. F. Hebard, R. P. Rairigh, J. G. Kelly, S. J. Pearton, C. R. Abernathy, S. N. G. Chu, and R. G. Wilson, *J. Phys. D* **37**, 511 (2004).
- ¹⁷S. O. Kucheyev, J. S. Williams, and S. J. Pearton, *Mater. Sci. Eng., R.* **33**, 51 (2001).
- ¹⁸N. Theodoropoulou, A. F. Hebard, M. E. Overberg, C. R. Abernathy, S. J. Pearton, S. N. G. Chu, and R. G. Wilson, *Phys. Rev. Lett.* **89**, 107203 (2002).
- ¹⁹J. Shi, J. M. Kikkawa, D. D. Awschalom, G. Medeiros-Ribeiro, P. M. Petroff, and K. Babcock, *J. Appl. Phys.* **79**, 5296 (1996).
- ²⁰A. Serres, M. Respaud, G. Benassayag, C. Armand, J. C. Pesant, A. Mari, Z. Lifiental-Weber, and A. Claverie, *Physica E (Amsterdam)* **17**, 371 (2003).
- ²¹H. H. Woodbury and G. W. Ludwig, *Phys. Rev.* **117**, 102 (1960).
- ²²H. Francois-Saint-Cyr, E. Anoshkina, F. Stevie, L. Chow, K. Richardson, and D. Zhou, *J. Vac. Sci. Technol. B* **19**, 1769 (2001).
- ²³B. E. Egamberdiev and M. Y. Adylov, *Tech. Phys. Lett.* **27**, 168 (2001).
- ²⁴H. Ohldag, V. Solinus, F. U. Hillebrecht, J. B. Goedkoop, M. Finazzi, F. Matsukura, and H. Ohno, *Appl. Phys. Lett.* **76**, 2928 (2000).
- ²⁵R. N. Bhatt, X. Wan, M. P. Kennett, and M. Berciu, *Comput. Phys. Commun.* **147**, 684 (2002).
- ²⁶H. Ohno, D. Chiba, F. Matsukura, T. Omiya, E. Abe, T. Dietl, Y. Ohno, and K. Ohtani, *Nature (London)* **408**, 944 (2000).
- ²⁷S. Das Sarma, E. H. Hwang, and A. Kaminski, *Phys. Rev. B* **67**, 155201 (2003).
- ²⁸L. Neel, *Ann. Geophys. (C.N.R.S.)* **5**, 99 (1949).
- ²⁹M. van Schilfgaarde and O. N. Mryasov, *Phys. Rev. B* **63**, 233205 (2001).